JOURNAL OF PROPULSION AND POWER
Vol. 9, No. 2, March–April 1993

Designing Hypersonic Inlets for Bow Shock Location Control

Mark J. Lewis*
University of Maryland, College Park, Maryland 20742

The desire to match the bow shock of a hypersonic vehicle to the lip of the engine cowl provides for a design constraint on the hypersonic forebody. For inviscid flow, it is shown that there is one particular wedge angle which provides for shock matching which is insensitive to steady-state changes in vehicle angle of attack, though it is not possible to match against changes in flight Mach number. The angle-of-attack sensitivity of a hypersonic boundary layer makes this matching process more difficult. Design rules for cowl matching with secondary shocks are presented, though it is shown that it is never possible to fix them against changes in angle of attack.

Nomenclature

H = shock layer height
M = Mach number
P = pressure
T = temperature
x = streamwise coordinate
α = angle of attack
β = shock angle to flow
γ = ratio of specific heats
δ^* = boundary-layer displacement thickness
θ = surface angle to flow
ρ = density
Φ = shock/surface relative angle
ϕ = boundary-layer slope

Subscripts
i = initial
t = total condition
w = wall value
0 = equilibrium value
1 = upstream or freestream
2 = downstream of first shock
3 = downstream of second shock

Introduction

CURRENT plans for a transatmospheric vehicle depend on the design of weight-saving engine-integrated airframes, in which the external vehicle surfaces act as components of the propulsion system. In particular, the aircraft forebody would serve as the engine compression surface, and the aftbody would act as the engine nozzle.[1] One of the implications of this integration is that the forebody must be properly shaped to provide efficient compression and to satisfy the requirements of the hypersonic engine. This work will explore some of the fundamental physical limitations in controlling the forebody flow, particularly the placement of the vehicle bow shock and various forebody design options available for controlling the bow shock placement. Important criteria for selecting the shock placement will be reviewed, and the role of viscous effects in determining the shock position will be addressed.

This work is motivated by the fact that control of the inlet bow shock, especially its location relative to the engine cowl lip, will be an important constraint in the design of an air-breathing hypersonic propulsion system. If the bow shock is placed too far away from the vehicle, there will be excessive wave drag. Because hypersonic vehicles will operate at thrust-to-drag ratios very close to unity, this additional cowl drag will be intolerable. Similarly, if the bow shock is swallowed into the cowl, deleterious reflections may propagate down through the engine. Another problem is that the impingement of the bow shock on the cowl lip may produce intense local heating.[2] These issues are demonstrated in Fig. 1, which shows the location of a bow shock and ramp shock on a hypersonic forebody, and demonstrates the relative position of those shocks.

For hypersonic cruise vehicles, it is desirable therefore, that the bow shock be approximately matched to the engine cowl, but controlled so that it does not make direct contact, whether in the steady state or as a transient. This leads to an interest in shock solutions that are fixed, relative to the inlet, against flight perturbations. Conversely, for accelerating vehicles, which will cover a wide range of Mach numbers, it will be impossible to fix the inlet shock. In this case, it is probably most desirable to minimize the contact time of the shock on the engine lip so as to avoid the highly destructive shock interaction heating. In that case, it is of interest to select a shock which will move into the engine rapidly in response to changes in Mach number. This leads to an interest in shock solutions with shock angles that are most sensitive to flight perturbations.

Shock Mismatch with Varying Flight Conditions

The bow shock matching problem is illustrated with the example of a two-dimensional wedge at hypersonic Mach numbers. Figure 2 presents the height of an oblique wedge shock at the end of a 30-m-long wedge set at angles of 5, 15, and 25 deg as a function of Mach number. Note that as Mach number increases, the separation between the shock and the wedge always decreases. Interestingly, below Mach 7, the 15-deg wedge shock is closer to the surface than that on the 5-deg wedge. Figure 3 shows the relative motion of a bow shock on the surface of a vehicle in inviscid flow, as measured

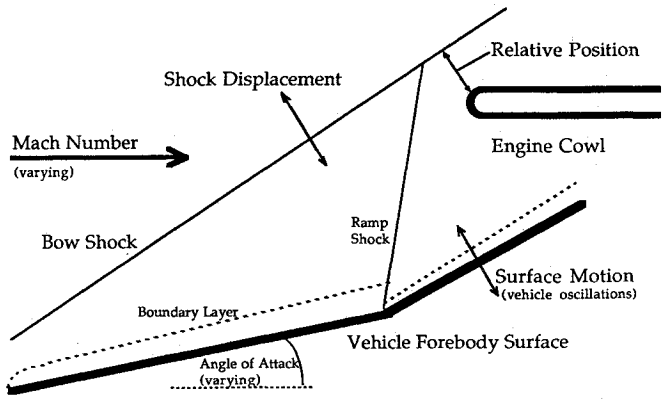

Fig. 1 Generic geometry for a hypersonic forebody showing shock location and relative position of shock over surface.

Received July 31, 1991; revision received Aug. 1, 1992; accepted for publication Aug. 21, 1992.

*Assistant Professor, Department of Aerospace Engineering. Member AIAA.

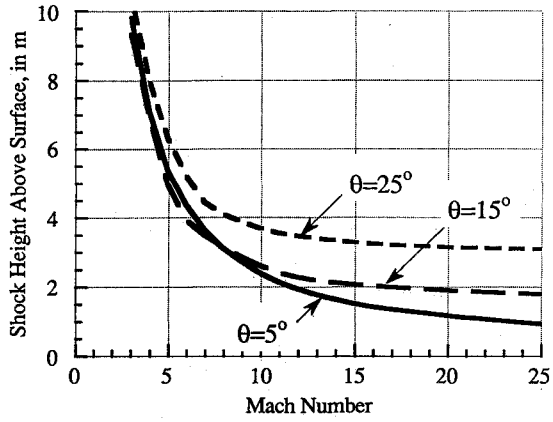

Fig. 2 Shock height above the surface at the end of a 30-m-long wedge as a function of Mach number, for wedge angles of 5, 15, and 25 deg.

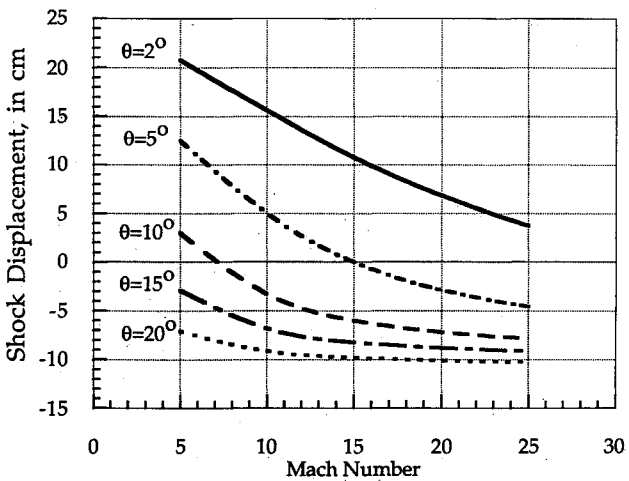

Fig. 3 Shock displacement with 1-deg increment in angle of attack on a 30-m wedge inlet.

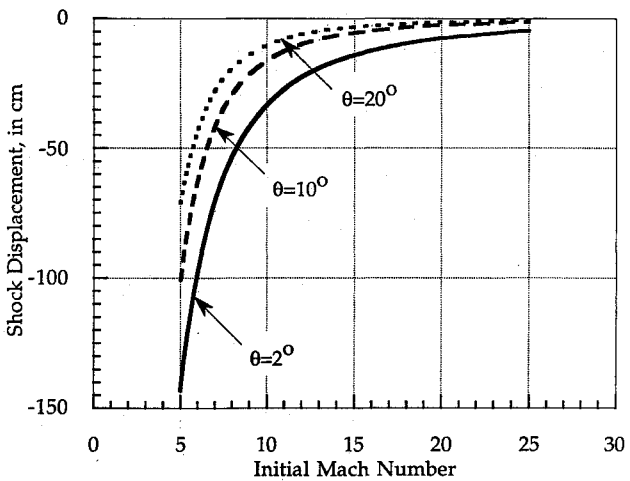

Fig. 4 Shock displacement with +1 increment in Mach number on a 30-m wedge inlet.

from that surface, subject to a 1-deg variation in the apparent surface angle of obliquity.

Typically, the angular deviation of the shock is within 10% of the surface angular displacement, so it would seem that the relative displacement problem should be insignificant. However, since a hypersonic vehicle will likely have a very long inlet surface to provide for adequate mass capture area, this seemingly small angular divergence can result in sizable linear displacements at the entrance to a hypersonic engine, as indicated by the values calculated in Fig. 3 for a 30-m-long wedge surface. It is likely that the diameter of the engine cowl lip of such vehicles will be measured in centimeters, so this shock displacement can be many times the cowl thickness.

A fascinating observation, and one of the keys to the primary topic of this work, is the fact that the sign of the relative shock displacement changes with Mach number. For instance, on the 5-deg wedge, an increase in surface angle causes the shock to move away from the surface at flight Mach number 5; at flight Mach number 15 there is almost no change in relative shock position, and at flight Mach number 20 the shock is displaced towards the surface when the surface angle increases. If this wedge were flying at Mach 15, the shock position would be relatively insensitive to changes in angle of attack. At high flight Mach numbers (but not, as will be shown later, for all Mach numbers) there is one specific wedge angle which guarantees that the motion of the shock is equal to the motion of the surface, and thus remains fixed relative to that surface.

Comparing the variation of displacement with Mach number for a given surface angle, it is clear that in each case increasing Mach number subtracts from the displacement of the shock. This has the interesting effect that the magnitude of displacement on a 2-deg wedge decreases with increasing Mach number, while that of a 15-deg wedge increases as Mach number increases.

This leads to another question about shock perturbation effects, namely that of how a shock moves in response to a small increase or decrease in Mach number. In other words, if an inlet is designed for perfect shock/cowl matching at one given design Mach number, what will happen when the vehicle is flown at a different Mach number? Figure 4 presents the shock displacement on wedges of various angles with a Mach number increment of 1. In other words, it presents the relative vertical motion of the shock as perceived by an observer on the wedge surface, resulting from an increase in freestream Mach number some initial value (e.g., $M = 5$) to 1+ that value (i.e., $M = 6$).

Figure 4 presents somewhat less surprising results than the displacements experienced with an increment in surface angle. As Mach number increases, the shock angle always decreases, so the shock always experiences a displacement in towards the surface. This displacement decreases as the surface wedge angle increases. Thus, increasing the wedge angle always decreases the displacement due to a change in Mach number. It should be noted that the above data is compiled for a fixed increment of +1 in Mach number; obviously, this represents a much larger fractional increment at lower Mach numbers than at higher ones, but even so, the results tend to confirm the Mach number independence principle, as variations in

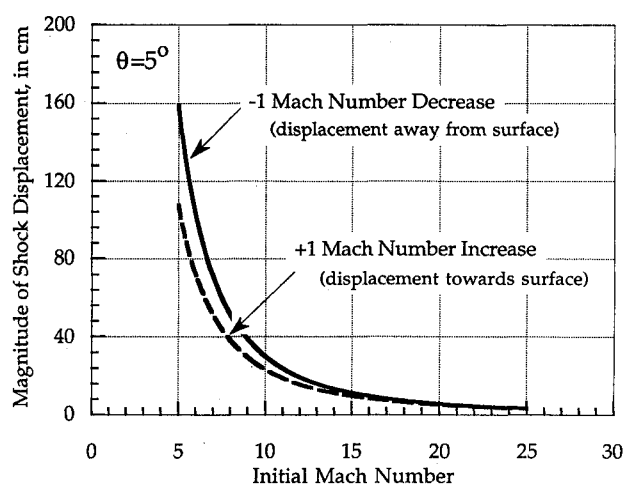

Fig. 5 Shock displacement with both +1 increment and −1 decrement in Mach number on a 30-m 5-deg wedge inlet. Note that incrementing Mach number displaces shock towards surface, decrementing moves it away.

displacement become much less noticeable at higher Mach numbers.

The relative displacement of the bow shock due to Mach number changes is not linear, as can be seen in Fig. 5. This figure presents the magnitude of the shock displacement relative to the design point, with both a +1 increment and −1 decrement in Mach number, on a 30-m-long wedge set at 5 deg to freestream. Note that the effect of increasing Mach number is always to drive the shock closer to the surface, while decreasing Mach number moves the shock away from the design point. Decreasing Mach number at lower Mach numbers results in substantially more deflection outward than increasing Mach number; starting at Mach 5, decreasing the Mach number to 4 displaces the shock 50% more than increasing Mach number to 6. At higher flight Mach numbers the displacement is more symmetrical.

From the point of view of engine integration requirements, the above results lead to the following inlet design questions:

1) Is there a specific wedge angle which minimizes relative shock displacement subject to a change in flight Mach number?

2) Is there a specific wedge angle which minimizes relative shock displacement subject to a change in that wedge angle?

3) What is the effect of adding an additional ramp downstream of the first wedge?

4) What is the effect of a thick hypersonic boundary layer on the matching process?

5) How significant is the influence of dynamic vehicle motion (i.e., high-frequency changes in angle of attack)?

These issues may be complicated by the presence of a thick hypersonic boundary layer, which is itself sensitive to changes in angle of attack and flight Mach number.[3]

Designing for Changes in Flight Mach Number

Controlling Shock Position

The familiar shock relations can be used to determine the effect of Mach number on the shock angle generated by a certain wedge angle.[4] The well-known relation between shock angle β, wedge angle θ, and M at a given value of γ can be written as

$$\theta = \beta - \Phi_{\text{relative}} \tag{1}$$

where

$$\Phi_{\text{relative}} = \tan^{-1}\{[(\gamma - 1)/(\gamma + 1)]\tan\beta + [2/(\gamma + 1)M^2 \sin\beta \cos\beta]\} \tag{2}$$

If the wedge is the surface of a vehicle, the effective surface angle θ has two components, one for the fixed vehicle geometry θ_{vehicle}, and the other for the effect of α:

$$(\theta_{\text{vehicle}} + \alpha) = \beta - \Phi_{\text{relative}} \tag{3}$$

A Mach-insensitive shock will be one in which

$$\frac{\partial\beta}{\partial M} = 0 \tag{4}$$

In the hypersonic limit $M \to \infty$, with small shock angles

$$\frac{\partial\beta}{\partial M} = \frac{1}{M^2\sqrt{[(\gamma + 1)/4]^2(M\theta)^2 + 1}} \tag{5}$$

Equation (5) shows that the shock motion due to changing Mach number can never be eliminated, but $d\beta/dM \to 0$ as $M \to \infty$ and, at small deflection angles, $\partial\beta/\partial M$ becomes smaller as β, and therefore, θ increases, which trends are indicated by Fig. 4. At very small surface angles, the change in shock angle with changing Mach number scales inversely with the square of the Mach number, which is the Mach wave limit; at larger surface angles, it scales inversely with the cube of Mach number times surface angle.

It may be concluded that there is no way to fix the relative shock displacement so that it is insensitive to Mach number changes; for a fixed inlet geometry, the bow shock will never match the cowl at off-design Mach numbers. However, these changes in displacement will be minimized at higher Mach numbers and larger surface angles. This latter fact will be important in considering multiple-ramp inlets.

Conversely, it was earlier suggested that it may be desirable to maximize, rather than minimize, the displacement of the bow shock of an accelerating hypersonic vehicle, so that at the point in its flight at which the bow shock passes across the engine cowl lip, that duration of high heating rate shock-shock interactions on the cowl is reduced. The above analysis suggests that this is best done by reducing the Mach number at which the shock crosses the inlet lip, and by using inlets with relatively shallow surface angles, such as multiple ramp designs with sidewall compression.

Resulting Variation in Pressure Ratio

Changes in Mach number will also lead to variations in the thermodynamic ratios across the bow shock. These can generally be accounted for by appropriate selection of flight altitude. In other words, if the Mach number increases and the pressure ratio rises, the vehicle can fly to higher altitudes where the lower ambient pressure can correct the engine inlet conditions. It is nonetheless of interest to discern the behavior of shock pressure ratio vs Mach number. This will be especially relevant to the later discussion of secondary ramps.

For hypersonic flow at small angles, the pressure ratio across a shock can be written as

$$(P_2/P_1) = 1 + [\gamma(\gamma + 1)/4](M\theta)^2 + \gamma(M\theta)^2\sqrt{[(\gamma + 1)/4]^2 + [1/(M\theta)^2]} \tag{6}$$

where M is the upstream Mach number.

The change in the pressure ratio due to a change in Mach number is

$$\frac{\partial}{\partial M}\left(\frac{P_2}{P_1}\right) = \frac{\gamma(\gamma + 1)[M\theta]\sqrt{(\gamma + 1)^2[M\theta]^2 + 16} + \gamma(\gamma + 1)^2[M\theta]^2 + 8\gamma}{2\sqrt{(\gamma + 1)^2[M\theta]^2 + 16}}\,\theta \tag{7}$$

For very large Mach number and moderate angle at $\gamma = 1.4$, $(\partial/\partial M)(P_2/P_1) \simeq 2.66[M\theta]\theta$; at very small angles and moderate Mach number, $(\partial/\partial M)(P_2/P_1) \simeq (0.59[M\theta]^2 + 1.68[M\theta] + 1.4)\theta$. Thus, thermodynamic changes associated with varying flight Mach number are increased at increasing Mach number or inlet ramp angle.

Designing for Changes in Angle-of-Attack

Controlling Shock Location

A similar analysis can be performed for the case of a change in angle of attack of a wedge with oblique angle, and the resulting variation in the shock displacement. It is of primary interest here to minimize relative shock motions on a hypersonic inlet so that the impact of vehicle maneuvering on engine flowfield is reduced.

As was pointed out in the discussion of Fig. 3, under certain circumstances there will be a given wedge angle such that a small change in that wedge angle does not change the relative position of the bow shock. This condition will be satisfied by setting

$$\frac{\partial\beta}{\partial\alpha} = 1 \tag{8}$$

where

$$\frac{\partial\alpha}{\partial\beta} = 1 - \frac{\partial\Phi_{\text{relative}}}{\partial\beta} \tag{9}$$

Taking the derivative of the relative angle $\Phi_{relative}$, defined in Eq. (2), with respect to shock angle

$$\frac{\partial \Phi_{relative}}{\partial \beta} \frac{[(\gamma - 1)/(\gamma + 1)(1/\cos^2\beta) + [2/(\gamma + 1)M^2][(1/\cos^2\beta) - (1/\sin^2\beta)]}{1 + \{[(\gamma - 1)/(\gamma + 1)]\tan\beta + [2/(\gamma + 1)M^2 \sin\beta \cos\beta]\}^2} \tag{10}$$

and setting

$$\frac{\partial \Phi_{relative}}{\partial \beta} = 0 \tag{11}$$

the "fixed-shock" solution is obtained for

$$\beta_{fixed} = \tan^{-1}\left[\frac{1}{\sqrt{1 + [(\gamma - 1)/2]M^2}}\right] \tag{12}$$

Note that the fixed shock angle is the arctangent of the square root of the ratio of static-to-total temperature in the flow. The normal Mach number corresponding to this fixed shock solution is

$$M_{normal} = M \sin\beta_{fixed} = \frac{M}{\sqrt{2 + [(\gamma - 1)/2]M^2}} \tag{13}$$

which approaches the constant hypersonic limiting value of $M_{normal} = \sqrt{2/(\gamma - 1)}$ at large M. For $\gamma = 1.4$, the hypersonic value is $M_{normal} = 2.236$. With the normal Mach number fixed, the thermodynamic jump across the shock is also determined:

$$\frac{P_2}{P_1} = -\frac{(\gamma^2 - 6\gamma + 1)M^2 + 4\gamma - 4}{(\gamma^2 - 1)M^2 + 4\gamma + 4} \tag{14}$$

$$\frac{\rho_2}{\rho_1} = \frac{(\gamma + 1)M^2}{2(\gamma - 1)M^2 + 4} \tag{15}$$

$$\frac{T_2}{T_1} = -\frac{2(\gamma^3 - 7\gamma^2 + 7\gamma - 1)M^4 + 4(3\gamma^2 - 10\gamma + 3)M^2 + 16(\gamma - 1)}{(\gamma^3 + \gamma^2 - \gamma - 1)M^4 + 4(\gamma^2 + 2\gamma + 1)M^2}$$

These ratios approach the hypersonic limits $T_2/T_1 \rightarrow 1.89$, $\rho_2/\rho_1 \rightarrow 3$, and $P_2/P_1 \rightarrow 5.67$ for $\gamma = 1.4$. Note that the density limit is exactly half the hypersonic density limit of a normal shock, and that, contrary to normal shock behavior, temperature and pressure do not go to infinity because the fixed shock solutions reduce shock angle as Mach number increases.

Table 1 presents the fixed-shock wedge angles and shock angle at $\gamma = 1.4$ for several Mach numbers. There is no fixed-shock wedge angle for Mach numbers below 1.581 at this value of γ, and the maximum fixed-shock wedge angle is 14.12 deg at Mach 3.572. There are no fixed-shock wedge angles for the strong shock solutions. The normal Mach number across the fixed shock is also shown. Figure 6 is a plot of the shock angle as a function of wedge angle through the range of Mach numbers.

The Mach number downstream of a shock can be written as

$$M_2 = \frac{1}{\sin\Phi_{relative}} \sqrt{\frac{(\gamma - 1)M_1^2 \sin^2\beta + 2}{2\gamma M_1^2 \sin^2\beta - (\gamma - 1)}} \tag{16}$$

where

$$\sin\Phi_{relative} = \frac{[(\gamma - 1)M_1^2 \sin^2\beta + 2]\tan\beta}{\sqrt{[(\gamma - 1)M_1^2 \sin^2\beta + 2]^2 \tan^2\beta + [(\gamma + 1)M_1^2 \sin^2\beta]^2}} \tag{17}$$

With the fixed-shock solution, this is equal to

$$M_2 = \sqrt{\frac{(\gamma - 1)M_1^2 + 2}{(-\gamma^2 + 6\gamma + 1)M_1^2 - 4(\gamma - 1)}} \frac{\sqrt{(\gamma^2 + 1)(\gamma - 1)M_1^6 + 2(5\gamma^2 - 6\gamma + 5)M_1^4 + 32[(\gamma - 1)M_1^2 + 1]}}{2[(\gamma - 1)M_1^2 + 2]} \tag{18}$$

which has a hypersonic limit of

$$M_2 \simeq \sqrt{\frac{\gamma^3 + \gamma^2 - \gamma - 1}{4(\gamma - 1)(-\gamma^2 + 6\gamma + 1)}} M_1 \tag{19}$$

With $\gamma = 1.4$, $M_2 = 0.440M_1$, and with $\gamma = 1.3$, $M_2 = 0.431M_1$. The fixed-shock solutions therefore provide a convenient estimate for the downstream Mach number, which is roughly linear with the flight Mach number.

Design Point Criteria

Given that the bow shock on a hypersonic inlet can be fixed against changes in angle of attack for one given Mach number, the question arises as to which Mach number to select as a design point. For sustained hypersonic cruise, the choice would naturally be the cruise Mach number, but for accelerating transatmospheric flight, such as for a single stage-to-orbit vehicle, the selection of a design point is less clear.

Obviously, the choice will depend in part on the allowable tolerance for shock mismatch at various flight speeds and engine operating conditions, so that only generalities can be stated here. Looking at Fig. 3, a 2-deg wedge will always be off-design across the range of transatmospheric Mach numbers. The 5-deg wedge is matched at Mach 10, and provides reasonable matching across the flight range. It is likely that the most critical point in the trajectory for engine operation would be in the vicinity of Mach 15, so it is probable that the most suitable transatmospheric design point would be at about 6 deg.

Controlling Thermodynamic Properties

It is also of interest to consider the design of an inlet which, in order to provide nearly constant pressure and temperature to the engine, minimizes changes in the shock thermodynamic properties, as opposed to the shock placement, subject to variations in angle of attack. Because the pressure and temperature jump across the shock are determined entirely by the normal Mach number, it is obvious that the shock with the minimum change in these properties will be the one which experiences the least change in absolute angle subject to a change in the surface angle.

A shock which does not change its angle as measured in the absolute frame would produce no net change in pressure and temperature subject to changes in angle of attack. Unfortunately, such a solution is not available, so the best solution will be one in which $\partial\Phi_{relative}/\partial\beta \rightarrow \infty$. Since the numerator of Eq. (10) must always be greater than 1, this condition can only be realized by setting

$$\frac{\gamma - 1}{\gamma + 1}\frac{1}{\cos^2\beta} + \frac{2}{(\gamma + 1)M^2}\left(\frac{1}{\cos^2\beta} - \frac{1}{\sin^2\beta}\right) \rightarrow \infty \tag{20}$$

This limit is approached as the shock angle goes to 0 or 90 deg, neither of which is possible for a real inlet. In the limit of small shock angle, we can write

$$\frac{\partial\beta}{\partial\Phi_{relative}} = \frac{(\gamma + 1)(M\beta)^2 + 4/M^2}{(\gamma - 1)(M\beta)^2 - 2} \tag{21}$$

At large Mach number, the tendency is for this to become independent of Mach number, which is the fixed shock limit.

Table 1 Fixed shock solutions at $\gamma = 1.4$

Mach no.	Shock angle, deg	Wedge angle, deg	Normal Mach no.	Temperature ratio	Pressure ratio
1.581	39.23	0.00	1.000	1.000	1.000
2	36.70	7.50	1.195	1.125	1.500
3.572	28.01	14.12	1.678	1.443	3.116
5	22.21	12.94	1.890	1.600	4.001
10	12.31	7.94	2.132	1.798	5.136
15	8.39	5.51	2.189	1.847	5.422
20	6.34	4.19	2.209	1.865	5.524
25	5.09	3.38	2.218	1.873	5.573
∞	0	0	2.236	1.889	5.667

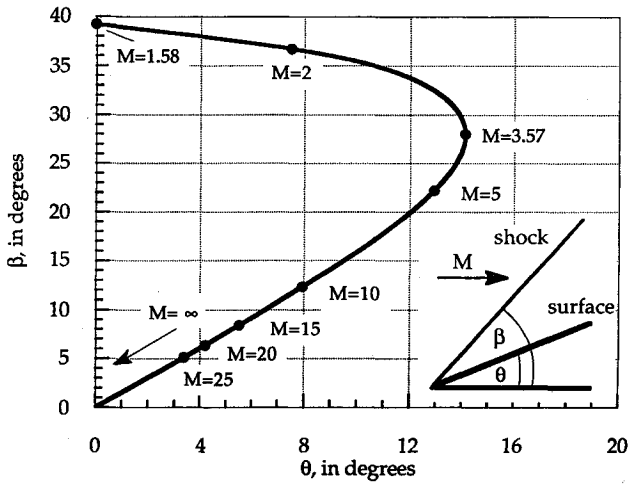

Fig. 6 Fixed shock solutions as a function of wedge angle and Mach number.

At any given Mach number, this function is minimized by setting the wedge angle to as small a value as possible. Thus, the fixed shock solutions may present too large a wedge angle if fixing of thermodynamic properties is desired. This will be explored further in the next section.

Properties of the Fixed-Shock Solutions

Thermodynamic Changes with Angle of Attack

With the fixed-shock solutions derived above, the relative location of the bow shock does not change for small variations in angle of attack. However, these solutions are still accompanied by changes in the thermodynamic properties across a shock, because the absolute value of shock angle is changing. In fact, these solutions are actually rather poor for purposes of minimizing the variation in thermodynamic properties subject to changes in angle of attack. Indeed, to minimize such variations, it would be desired to have a bow shock which remains fixed in the absolute frame subject to changes in angle of attack.

For the fixed-shock solutions, the change in thermodynamic properties can be calculated as a function of changing angle of attack. Pressure is likely to be the most important property to control in order to maintain engine combustion. Recalling that the pressure across a shock is

$$(P_2/P_1) = 1 + [2\gamma/(\gamma + 1)](M^2 \sin^2\beta - 1) \qquad (22)$$

we can solve for the change due to variations in angle of attack by noting that the fixed-shock solutions are defined such that $\partial/\partial\alpha = \partial/\partial\beta$, and substituting for the value of β_{fixed}, as

$$\frac{\partial}{\partial\alpha}\left(\frac{P_2}{P_1}\right) = \frac{2\gamma}{\gamma + 1} M^2 \sin 2\beta \qquad (23)$$

$$= \frac{8\gamma\sqrt{1 + [(\gamma - 1)/2]M^2}}{4\gamma + 4 + (\gamma^2 - 1)M^2} M^2 \qquad (24)$$

The relative change in pressure ratio can be written by dividing this by Eq. (14)

$$\frac{\dfrac{\partial}{\partial\alpha}\left(\dfrac{P_2}{P_1}\right)}{\dfrac{P_2}{P_1}} = -\frac{8\gamma M^2\sqrt{1 + \dfrac{\gamma - 1}{2}M^2}}{(\gamma^2 - 6\gamma + 1)M^2 + 4(\gamma - 1)} \qquad (25)$$

In the hypersonic limit

$$\frac{\dfrac{\partial}{\partial\alpha}\left(\dfrac{P_2}{P_1}\right)}{\dfrac{P_2}{P_1}} \simeq -\frac{8\gamma\sqrt{\dfrac{\gamma - 1}{2}}}{\gamma^2 - 6\gamma + 1} M \qquad (26)$$

Thus, the fractional change in pressure ratio across a fixed shock increases linearly with Mach number, so these solutions have the undesirable effect of amplifying thermodynamic variations at higher velocities. For $\gamma = 1.4$ and fixed ambient pressure, this can be written as

$$\frac{\partial P_2}{P_2} = 0.921M\,\partial\alpha \qquad (27)$$

A 1-deg change in angle of attack will therefore produce a fractional change in pressure behind the bow shock of $\partial P_2/P_2 = 0.016M$. At Mach 5, this will represent an 8% change in pressure; at Mach 10, a 16% change; and at Mach 20, a 32% fractional change per degree. This may have significant consequences for the combustion process.[5] Decreasing γ reduces the value of the constant of proportionality; for $\gamma = 1.3$ the constant is 0.788.

Similarly, the change in temperature is also approximately linear with Mach number in the hypersonic limit. Taking the derivative of the temperature ratio with respect to angle of attack

$$\frac{\partial}{\partial\alpha}\left(\frac{T_2}{T_1}\right) = \frac{4(\gamma - 1)(\gamma M^4 \sin^4\beta + 1)}{(\gamma + 1)^2 M^2 \sin^2\beta \tan\beta} = \frac{2(\gamma - 1)[(\gamma + 1)M^2 - 4M + 4][(\gamma + 1)M^2 + 4M + 4]\sqrt{1 + [(\gamma - 1)/2]M^2}}{(\gamma + 1)^2 M^2[(\gamma - 1)M^2 + 4]} \qquad (28)$$

and assuming large Mach number

$$\frac{\dfrac{\partial}{\partial\alpha}\left(\dfrac{T_2}{T_1}\right)}{\dfrac{T_2}{T_1}} \simeq -\frac{\sqrt{\dfrac{\gamma - 1}{2}}(\gamma^3 + \gamma^2 - \gamma - 1)}{(\gamma^3 - 7\gamma^2 + 7\gamma - 1)} M \qquad (29)$$

At $\gamma = 1.4$

$$\frac{\partial T_2}{T_2} = 0.474M\,\partial\alpha \qquad (30)$$

and for $\gamma = 1.3$ the constant is 0.401. A 1-deg change in angle of attack produces a fractional change of $\partial T_2/T_2 = 0.009M$, which is 4% at Mach 5, 8% at Mach 10, and 16% at Mach 20. Note that the temperature change is less sensitive than pressure, but it is likely that pressure will be more important in maintaining combustion.

Comparison to Minimum Pressure Variation Solutions

It is of interest to compare the pressure variations associated with angle-of-attack changes using the fixed-shock solution to those of the minimum pressure variation shock solution. At

the minimum, the wedge angle approaches zero, so

$$\frac{\partial}{\partial\alpha}\left(\frac{P_2}{P_1}\right) = \frac{\gamma M^2}{\sqrt{M^2-1}} \tag{31}$$

$$\frac{\partial}{\partial\alpha}\left(\frac{T_2}{T_1}\right) = \frac{(\gamma-1)M^2}{\sqrt{M^2-1}} \tag{32}$$

These relations are derived by taking the Mach wave limit of the shock solutions, as performed in Ref. 6. For $\gamma = 1.4$ and large Mach number, $(\partial/\partial\alpha)(P_2/P_1) = 1.4M$ and $(\partial/\partial\alpha)(T_2/T_1) = 0.4M$, vs $(\partial/\partial\alpha)(P_2/P_1) = 5.22M$ and $(\partial/\partial\alpha)(T_2/T_1) = 0.90M$ for the fixed-shock solution. Since the pressure and temperature rise in the small angle solution approach unity, the fractional increase in pressure due to a change in angle of attack is 1.52 times greater than for the fixed-shock solution. In fact, there is no shock solution for minimum fractional pressure change; increasing the wedge angle always decreases this quantity.

Secondary Ramps and Compression Surfaces

Secondary Shock Matching with Varying Angle of Attack

As found above, the fixed-shock solutions provide temperature ratios of approximately 1.89 in the hypersonic limit. For typical transatmospheric vehicle flight operations, it will be desired to raise ambient temperatures of approximately 220–320 K to 1000 K to initiate combustion, requiring an inlet temperature rise of between 3 and 5. If the fixed-shock solution is used for the bow, it is clear that secondary ramps or compression surfaces will have to be used along the forebody to further compress the incoming flow.

It is tempting to ask if these secondary shocks can be fixed on the cowl lip, just as the bow shock can. The answer to this is no, for reasons already stated above. The secondary ramps do not see a change in surface angle when the vehicle angle of attack changes; the first bow shock always turns the flow parallel to the forebody surface. Rather, secondary surfaces see a change in incoming Mach number as vehicle angle of attack changes, and it was shown that a shock cannot be fixed against changes in incoming Mach number.

Therefore, it is of interest to determine the change in Mach number coming through one of these fixed shocks in response to change in angle of attack. This is done by taking the derivative of Eq. (16) with respect to β, noting that the fixed-shock solution is such that this is also the derivative with respect to α, and further noting that $\partial\Phi_{\text{relative}}/\partial\alpha = 0$.

$$\frac{\partial M_2}{\partial\alpha} = -\left\{\frac{(\gamma+1)^2(\gamma-1)M_1^4 + 4(\gamma+1)^2M_1^2}{4[-(\gamma^2-6\gamma+1)M_1^2 - 4(\gamma-1)]^{3/2}}\right\} \times \sqrt{\frac{[(\gamma+1)^2M_1^4 + 8(\gamma-1)M_1^2 + 16}{(\gamma-1)M_1^2+2}} \tag{33}$$

which in the hypersonic limit, approaches

$$\frac{\partial M_2}{\partial\alpha} = -\frac{(\gamma+1)^3\sqrt{\gamma-1}}{4(-\gamma^2+6\gamma-1)^{3/2}}M_1^2 \tag{34}$$

so that $\partial M_2/\partial\alpha = -0.172M_1^2$ at $\gamma = 1.4$ and $\partial M_2/\partial\alpha = -0.144M_1^2$ at $\gamma = 1.3$. Note that station 2 represents conditions just downstream of the first bow shock. At higher Mach numbers, the change in downstream Mach number with a variation in angle of attack will be more significant. Also note that Mach number downstream of the first shock is decreasing as angle of attack increases, because the shock is becoming stronger.

A second ramp on the forebody surface will therefore respond to the change in angle of attack because it will perceive a change in upstream Mach number. With the chain rule and the results of Eq. (5), the angle of the secondary ramp shock, β_2, can be related to the change in Mach number coming through the first inlet shock: $(\partial\beta_2/\partial\alpha) = (\partial\beta_2/\partial M_2)(\partial\beta_2/\partial M_2)$, which is the product of Eqs. (33) and (5). In the hypersonic limit, this becomes $(\partial\beta_2/\partial\alpha) = -3.365/M_1\theta_2$ at $\gamma = 1.4$; and $(\partial\beta_2/\partial\alpha) = -3.128/M_1\theta_2$ at $\gamma = 1.3$, where θ_2 is the angle of the ramp. The negative sign shows that the secondary ramp shock motion cannot be eliminated relative to the inlet surface. Increasing flight Mach number or the angle of the secondary ramp will decrease the relative motion.

This leads to the following design rule: although it is impossible to eliminate the motion of the shock on a secondary ramp on a hypersonic inlet (as can be done with the bow shock), that motion can be minimized by using as large a ramp angle as possible. In other words, for a given compression ratio, two ramp inlets will have less shock motion than three or more ramps. A hypersonic inlet which is designed to minimize shock displacement subject to angle of attack variations, will have an initial ramp angle at the fixed-shock value and one additional subsequent ramp which completes the compression.

Pressure Change on a Secondary Ramp with Angle of Attack

Equation (7) showed the change of shock pressure ratio as a function of varying Mach number. Since the effect of varying angle of attack is to change Mach number downstream of the fixed shock, this same equation can be used to determine the pressure ratio changes on a secondary ramp. Note that to use the hypersonic assumption, flow behind the bow shock must still be hypersonic, which is strictly applicable at flight Mach numbers in excess of about 11. Once again using the chain rule, the change in overall pressure ratio across the inlet, between station 3 behind the second ramp shock, and the freestream conditions, is

$$\frac{\partial}{\partial\alpha}\left(\frac{P_3}{P_1}\right) = \left[\frac{P_2}{P_1}\right]\frac{\partial M_2}{\partial\alpha}\frac{\partial}{\partial M_2}\left(\frac{P_3}{P_2}\right) + \left[\frac{P_3}{P_2}\right]\frac{\partial}{\partial\alpha}\left(\frac{P_2}{P_1}\right) \tag{35}$$

Substituting the values for the fixed-shock solutions derived above at $\gamma = 1.4$, the overall pressure ratio will be sensitive to angle of attack changes as

$$\frac{\partial}{\partial\alpha}\left(\frac{P_3}{P_1}\right) = 3.44M_1^3\theta_2^2 + 5.22M_1 + 4.38M_1\sqrt{1+\frac{13.89}{(M_1\theta_2)^2}} \tag{36}$$

where the pressure ratio on the ramp has been related to the ramp angle with Eq. (6).

Note that increasing the ramp angle θ_2 increases the sensitivity of the overall inlet pressure ratio to changes in angle of attack. This sensitivity increases with the cube of the flight Mach number. In order to design an inlet with less pressure sensitivity to changes in attitude, it is best to use many subsequent ramps at shallow angles. This conclusion is consistent with the earlier finding that larger ramp angles lead to less relative shock motion; a shock which is less resistant to changing its angle will experience a greater change in pressure ratio as the upstream Mach number is increased. Thus, a decision must once again be made between the desire for controlling shock position and minimizing the change in thermodynamic fluctuations subject to variations in angle of attack.

Isentropic Compression Surface

Instead of a second shock, a hypersonic inlet may have an isentropic compression surface following the bow shock. We can compare changing angle of attack with ramp inlet to that of an isentropic compression surface. On such a surface, the

change in Mach number is a function only of the turning angle

$$\Delta\theta = \int_{M_1}^{M_2} \frac{\sqrt{M^2 - 1}}{1 + [(\gamma - 1)/2]M^2} \frac{dM}{M} \tag{37}$$

An infinitesimal change in upstream M_1 produces a corresponding change in downstream M_2 since $\Delta\theta$ cannot change

$$\frac{dM_2}{dM_1} = \frac{M_2\{1 + [(\gamma - 1)/2]M_2^2\}\sqrt{M_1^2 - 1}}{M_1\{1 + [(\gamma - 1)/2]M_1^2\}\sqrt{M_2^2 - 1}} \tag{38}$$

Where it is assumed that the flow is still isentropic (i.e., no strong shocks have formed.) Since the flow is isentropic, the pressure ratio is

$$\frac{P_2}{P_1} = \left\{\frac{1 + [(\gamma - 1)/2]M_1^2}{1 + [(\gamma - 1)/2]M_2^2}\right\}^{\gamma/(\gamma-1)} \tag{39}$$

The derivative of pressure is

$$\frac{d}{dM_1}\left(\frac{P_2}{P_1}\right) = \frac{\gamma(M_1^2\sqrt{M_2^2 - 1} - M_2^2\sqrt{M_1^2 - 1})}{M_1\{1 + [(\gamma - 1)/2]M_1^2\}\sqrt{M_2^2 - 1}} \frac{P_2}{P_1} \tag{40}$$

In the hypersonic limit

$$\frac{d}{dM_1}\left(\frac{P_2}{P_1}\right) \simeq \frac{2\gamma[1 - (P_2/P_1)^{-(\gamma-1)/2\gamma}]}{(\gamma - 1)M_1} \frac{P_2}{P_1} \tag{41}$$

With $\gamma = 1.4$

$$\frac{d}{dM_1}\left(\frac{P_2}{P_1}\right) \simeq \frac{7}{M_1}\left(\frac{P_2}{P_1} - \frac{P_2^{0.857}}{P_1}\right) \tag{42}$$

In most practical cases, the pressure change due to changes in angle of attack on the isentropic inlet will be approximately equal to that generated on a secondary ramp shock, to within 20%. The bow shock change will, of course, be the same in both cases. This means that minimizing pressure variations downstream cannot be used to select between a ramp and isentropic compression. This is demonstrated in Fig. 7, which presents the pressure derivative with respect to changing Mach number caused by a variation in angle of attack for both a secondary ramp and an isentropic inlet, at various pressure rations. Note that the isentropic solution is smaller at lower pressure ratios, and slightly larger at higher pressure ratios, but always by an insignificantly small margin.

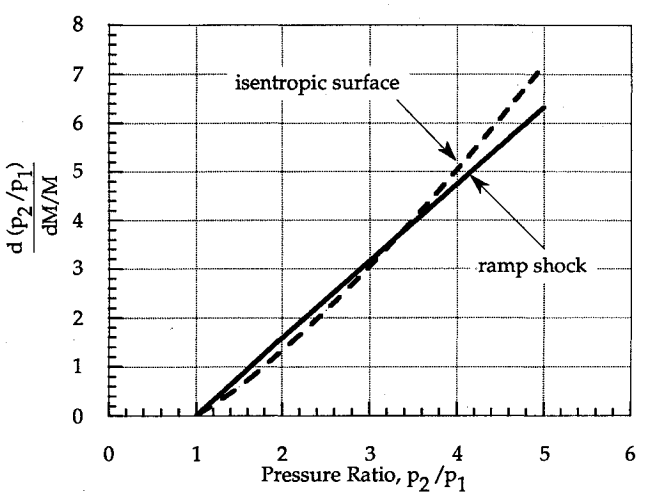

Fig. 7 Pressure derivative for a ramp and isentropic inlet at Mach 15.

Viscous Influences on Shock Matching

In viscous hypersonic flow, the shock position is no longer set by the shock angle alone, but also by the boundary-layer thickness.[7] Hypersonic laminar boundary layers will be thick, perhaps representing up to 25% of the shock layer height.[8] The boundary-layer thickness is sensitive to angle of attack, varying roughly in proportion to angle of attack at wedge angles in excess of a few degrees. Therefore, the boundary-layer thickness must be considered in matching the shock to the inlet lip, and changes in that boundary-layer thickness must be accounted for if the shock is to remain fixed. At large Mach number and small angle of attack, increasing angle of attack results in the shock moving away from the surface, but in general, this effect will not be sufficient to cancel the effects of decreasing boundary-layer thickness.

With the simplification that boundary-layer thickness is inversely proportional to the wedge angle, the expression for the boundary-layer height as a function of angle of attack compared to some initial condition at apparent wedge angle $\alpha_i + \theta$ is

$$\delta(\alpha) = \delta_i[(\alpha_i + \theta)/(\alpha + \theta)] \tag{43}$$

The angular displacement between the top of the boundary layer and the surface, defined here as ϕ, is

$$\tan\phi = \frac{\delta_i}{x}\frac{\alpha_i + \theta}{\alpha + \theta} \tag{44}$$

where $\tan\phi \simeq \phi$ in the small-angle approximation. The derivative of ϕ with respect to α is then

$$\frac{\partial\phi}{\partial\alpha} = -\frac{\delta_i}{x}\frac{\alpha_i + \theta}{(\alpha + \theta)^2} \tag{45}$$

This added angular displacement due to boundary-layer thickness changes the apparent wedge angle, because the top of the boundary layer, not the vehicle surface, defines the downstream flow angle. Equation (3) is modified to include ϕ in the shock angle relation of

$$(\theta_{\text{vehicle}} + \alpha + \phi) = \beta - \Phi_{\text{relative}} \tag{46}$$

where Φ_{relative} is now the angular displacement between the shock and the top of the boundary layer. The fixed-shock solution will be one in which

$$\frac{\partial\alpha}{\partial\beta} = 1 - \frac{\partial\Phi_{\text{relative}}}{\partial\beta} - \frac{\partial\phi}{\partial\beta} = 1 \tag{47}$$

so that

$$\frac{\partial\Phi_{\text{relative}}}{\partial\beta} + \frac{\partial\phi}{\partial\beta} = 0 \tag{48}$$

which is the condition that changes in the angular displacement of the top of the boundary layer are identically cancelled by changes in the relative angular displacement between the boundary layer and the shock.

When this condition is satisfied, $\partial\alpha/\partial\beta = 1$ and we can write

$$\frac{\partial\phi}{\partial\beta} = -\frac{\delta_i}{x}\frac{\alpha_i + \theta}{(\alpha + \theta)^2} \tag{49}$$

For small displacements, $\alpha + \theta = \beta - \Phi_{\text{relative}} - \delta_i/x$, and the derivative of the angular displacement of the boundary layer with respect to the shock angle is

$$\frac{\partial\phi}{\partial\beta} = -\frac{\delta_i/x}{\beta - \Phi_{\text{relative}} - \delta_i/x} \tag{50}$$

For a given value of δ_i/x at M, the fixed shock has angle β which satisfies

$$\frac{[(\gamma-1)/(\gamma+1)](1/\cos^2\beta)+[2/(\gamma+1)M^2][(1/\cos^2\beta)-(1/\sin^2\beta)]}{1+\{[(\gamma-1)/(\gamma+1)]\tan\beta+[2/(\gamma+1)M^2\sin\beta\cos\beta]\}} - \frac{\delta_i/x}{\beta-\tan^{-1}\{[(\gamma-1)/(\gamma+1)]\tan\beta+[2/(\gamma+1)M^2\sin\beta\cos\beta]\}-\delta_i/x}=0 \quad (51)$$

In fact, δ_i/x will vary all along the surface, so the fixed-shock solution will also vary down the surface. Thus, even though the shock can be fixed against changes in the conditions at the inlet lip, changes in wedge angle upstream of the lip will move the shock and the fixed condition cannot be satisfied perfectly.

There is no closed-form solution for Eq. (51), but with a small angle approximation (shock angles must be small in the hypersonic regime to avoid unreasonable temperature and pressure rises), considerable simplification is possible:

$$\frac{[(\gamma-1)/(\gamma+1)]-[2/(\gamma+1)M^2\beta^2]}{1+\{[(\gamma-1)/(\gamma+1)]\beta+[2/(\gamma+1)M^2\beta]\}^2} - \frac{\delta_i/x}{\beta-\tan^{-1}\{[(\gamma-1)/(\gamma+1)]\beta+[2/(\gamma+1)M^2\beta]\}-\delta_i/x}=0 \quad (52)$$

Equation (52) has been used to solve for the fixed-shock wedge angle and shock angle, and the results are presented in Fig. 8. Fixed-shock conditions were determined as a function of Mach number at $\gamma = 1.4$, for a shock layer without a boundary layer (corresponding to Table 1), with 2% relative boundary-layer thickness, and with 5% relative boundary-layer thickness, referenced to the height of the shock. Above 5% boundary-layer thickness, the required shock angle is too large for the small angle approximation to be valid. Above 20% thickness, no fixed shock solution can be found with even the full solution. That is because the inviscid shock motion is no longer of sufficient magnitude to cancel boundary-layer motions, which scale with boundary-layer thickness.

The boundary layer tends to raise the fixed-shock angle to unreasonable large values. For instance, with 2% relative boundary-layer thickness, the fixed-shock angle at Mach 20 has jumped from 6.34 deg, for the inviscid case, to 9.99 deg. This, in turn, will yield a normal Mach number of 3.470, with a temperature ratio across the shock of 3.274. This is unacceptable for typical ambient conditions; a two-shock inlet would raise a 300 K ambient flow to 3216 K, which is too high for combustion to occur.

It can be concluded that it is possible to cancel out the effect of angle of attack on boundary-layer thickness on the shock motion by selecting an appropriate wedge angle, for relative boundary-layer thickness of less than a few percent. The presence of a thick boundary layer, in excess of 5% of the shock layer, will mean that it is impossible to keep the shock fixed on the inlet lip without some active control or variable geometry.

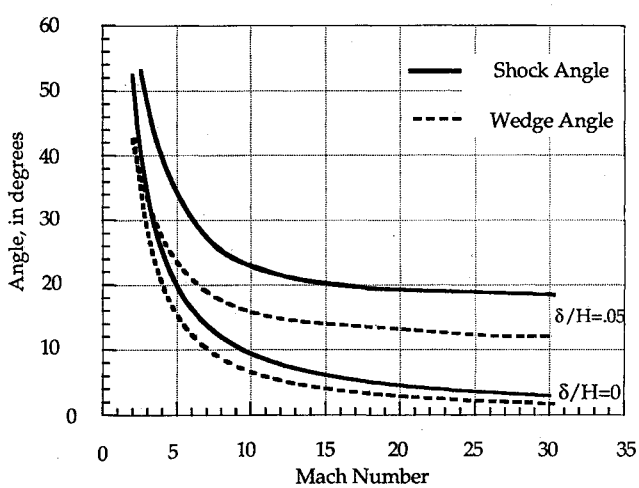

Fig. 8 Fixed-shock solutions as a function of ratio of boundary-layer thickness to shock layer height.

Conclusions

Matching a bow shock to an engine inlet cowl introduces an important design constraint for a hypersonic forebody. In the inviscid limit, and for a forebody with very small boundary layer, this matching can be accomplished such that the shock location is fixed relative to the engine cowl, subject to changes in angle of attack. Such fixing becomes more difficult with a thick boundary layer, the thickness of which varies with vehicle angle of attack. It is not possible to fix a shock against changes in Mach number, which means that an inlet will have to be designed with variable geometry, or flown at a given design Mach number.

From the design point of view, the importance of these results rests with the cowl's tolerance of shock mismatch, and the engine's ability to operate with varying inlet flow conditions. Given that such variations must be limited as much as possible, it is suggested that an inlet be designed with the fixed shock criterion where possible under boundary-layer conditions, matched at a selected cruise or critical flight Mach number. On design, the shock is fixed against perturbations in attitude, which are more likely than variations in flight Mach number. This design condition will not provide adequate compression in most cases, and so secondary compression must be accomplished on the inlet.

If a secondary ramp inlet is to be used, it is best to use only one other ramp in order to control shock position. Multiple ramp inlets will always have less control over the shock position, because the shock displacement decreases with increasing shack angle and Mach number. This shock control design condition is not an absolute, but must be balanced against drag constraints on the vehicle. It was shown that for an isentropic compression, which has no shock to begin with, the thermodynamic conditions vary about the same as those of a ramp shock subject to changes in angle of attack.

All of this is to control against steady-state, or low-frequency changes in the vehicle angle of attack. It has been found that high-frequency variations tend to be transmitted directly to the bow shock, so that the shock motion follows the surface motion quite closely.[9] Even with a thick boundary layer, which has the potential for amplifying surface motion, no important mismatches will be seen at reasonable oscillatory frequencies. Thus, the inlet design need only address the steady-state variations.

Acknowledgments

A portion of this work was supported by the Charles Stark Draper Laboratory, under Contract DL-H-261843, supervised by Phil Hattis. The author would like to thank M. Martinez-Sanchez and D. H. Hastings of the MIT Department of Aeronautics and Astronautics, Fred Billig of the Johns Hopkins Applied Physics Laboratory, and Henry Nagamatsu, of Rensselaer and Polytechnic Institute, for helpful suggestions and insights.

References

[1]Waltrup, P., "Liquid-Fueled Supersonic Combustion Ramjets: A Research Perspective," *Journal of Propulsion and Power*, Vol. 3, No. 6, 1987, pp. 515–525.

[2]Holden, M. S., Wieting, A. R., Moselle, J. R., and Glass, C., "Studies of Aerothermal Loads Generated in Regions of Shock/Shock Interaction in Hypersonic Flow," AIAA Paper 88-0477, Jan. 1988.

[3]Lewis, M. J., "The Prediction of Inlet Flow Stratification and Its Influence on the Performance of Air-Breathing Hypersonic Propulsion Systems," Ph.D. Dissertation, MIT Dept. of Aeronautics and Astronautics, Cambridge, MA, 1988.

[4]Anderson, J. D., *Modern Compressible Flow with Historical Perspective*, McGraw-Hill, New York, 1982, p. 90.

[5]Rogers, C. R., and Schexnayder, C. J., "Chemical Kinetic Analysis of Hydrogen-Air Ignition and Reaction Times," NASA TP-1856, July 1981.

[6]Liepmann, H. W., and Roshko, A., *Elements of Gasdynamics*, Wiley, New York, 1957, p. 92.

[7]Bertram, M. H., and Blackstock, T. A., "Some Solutions to the Problem of Predicting Boundary-Layer Self-Induced Pressures," NASA TN-798, April 1961.

[8]Lewis, M. J., and Hastings, D. E., "Some Consequences of Flow Non-Uniformities on the Forebody of a Trans-Atmospheric Vehicle," AIAA Paper 88-3057, July 1988.

[9]Lewis, M. J., Surline, Y., and Anderson, J. D., "An Analytical and Computational Study of Unsteady Shock Motion on Hypersonic Forebodies," *Journal of Aircraft*, Vol. 28, No. 8, 1991, pp. 532–539.